IEEE Access
Multidisciplinary | Rapid Review | Open Access Journal

Received September 15, 2021, accepted September 20, 2021, date of publication September 22, 2021,
date of current version October 1, 2021.

Digital Object Identifier 10.1109/ACCESS.2021.3114785

Hybrid Energy Storage System Based on Li-Ion and Li-S Battery Modules and GaN-Based DC-DC Converter

ANDER AVILA, MATTIN LUCU, (Member, IEEE), ASIER GARCIA-BEDIAGA, (Member, IEEE), UNAI IBARGUREN, IÑIGO GANDIAGA, AND ALEJANDRO RUJAS
Ikerlan Technology Research Centre, Basque Research and Technology Alliance (BRTA), 20500 Arrasate-Mondragón, Spain
Corresponding author: Ander Avila (aavila@ikerlan.es)

This work was supported by the European Union's Horizon 2020 Research and Innovation Programme under Grant 770019.

ABSTRACT Lithium-ion (Li-ion) batteries are still the best technology to power the Electric Vehicle (EV), due to their high power and energy density. However, the use of these batteries can be limited in cars with a high demand for peak power and very high energy density. One way to improve the performance of the Li-ion battery and reduce its weight is to associate this battery with another technology of higher specific energy as a second energy source, e.g. Lithium-sulfur (Li-S). The development of Hybrid Energy Storage Systems (HESSs) is a promising solution optimizing the energy management of EVs. In this paper, we present experimental results obtained with a high specific energy and power capability HESS prototype, composed of i) a Lithium-Titanate-Oxide battery to ensure high power capabilities, ii) a Li-S battery to improve specific energy, and iii) a power converter based on Gallium Nitride (GaN) devices to link both battery modules, minimizing at the same time system weight, volume and power losses. The developed GaN-based power converter achieves high efficiency (96.5%) operating at 300 kHz with a reduced size (0.4 L). Besides, the behavior of the developed HESS prototype is experimentally evaluated under standard automotive profiles, for different driving scenarios. The HESS prototype achieves an increase of energy density and specific energy of +5.56% and +28.21%, respectively, compared to a battery system composed only of Li-ion cells. The limitation of the developed system for automotive application are highlighted, and the critical research needs are clearly identified to accelerate the implementation of such systems on commercial EV solutions.

INDEX TERMS Li-S, DC-DC, hybrid energy storage system, electric vehicle, gallium nitride.

I. INTRODUCTION

According to recent data [1], the electrification of transportation is key to reduce the greenhouse gas emissions. Some of the main challenges for the wide adoption of Electric Vehicles (EVs) are to extend the range of the vehicle and reduce the time required to fully charge the battery. This implies the development of battery systems which present at the same time an increased energy density, specific energy, and power capability [2].

To achieve such objectives, the global research in battery systems focuses on several paths. On the one hand, new battery chemistries are being developed trying to reach both energy and power requirements at cell level [3]. On the other hand, Hybrid Energy Storage Systems (HESSs) typically combining two cell technologies are being proposed, allowing to achieve energy and power requirements at system level [4], [5]. Although several cell technologies are already commercially available to reach high power capabilities (e.g. supercapacitors [6] and Lithium-titanate-oxide batteries [7]), the development of cell chemistries, presenting increased energy density and specific energy, remains challenging. Among the different possible solutions, only Li-metal anode technologies seem to be able to provide a satisfying improvement in the short- middle-term [8]. Particularly, Lithium-sulfur (Li-S) technology is considered as a promising candidate due to its outstanding theoretical gravimetric capacity [9]. Such technology, which typically

The associate editor coordinating the review of this manuscript and approving it for publication was Rocco Giofrè.

combines Lithium-metal anode with a sulfur-based cathode [10], is gaining attention within the battery research community [11], [12] and early commercial products were already introduced in the market in the past few years.

An additional challenge in HESS solutions is that power electronics interfaces are typically required to connect both battery technologies, and implement energy management strategies to ensure the optimal use of both battery technologies [5], [13], [14]. Such additional circuitry could compromise the energy density and specific energy improvements achieved through battery chemistry hybridization. Therefore, the development of reduced volume and weight power converters is of high importance [5], [15]–[17]. Within this context, the use of wide-bandgap semiconductors such as Gallium Nitride (GaN) devices presents an increased interest. In fact, their low conduction resistance and high-frequency operation characteristics allows to derive high efficiency and reduced size power converters [15], [17]–[19], improving in turn the efficiency, energy density and specific energy at system level.

Several HESS solutions were already proposed in the literature [5], [20]–[22]. Nevertheless, most of them were focused on improving the power capability of conventional Li-ion technology through the incorporation of supercapacitors, neglecting the need to improve the energy requirements of state-of-the-art systems. Moreover, most papers only involved simulation results of system behavior, while experimental results are unusual in the literature. Finally, no special attention was paid on the impact of the power converters themselves on system energy density and specific energy.

The present study is based on the analysis of the experimental results of a HESS prototype with high energy and power performance under different automotive profiles. The HESS system is composed of a LTO anode Lithium battery that guarantees high power requirements and a module of the novel Li-S technology with the aim of increasing the specific energy. A bidirectional power converter based on GaN semiconductors was developed to connect both batteries.

Therefore, the present paper aims to bring several contributions to the literature:

i) The proposed HESS integrates the latest Li-S technology, which enables to increase the energy density and specific energy of the system.
ii) The impact of the power converter stage is considered and minimized through the development of high-efficiency and reduced size GaN-based power converter.
iii) The developed HESS prototype is experimentally validated under different EV profiles, and the obtained results are thoroughly evaluated.

This paper is structured as follows, Section II describes the main characteristics of the selected Li-ion and Li-S cell and modules, as well as the adopted hybridization topology. Section III emphasizes on the performance evaluation and experimental validation of the developed GaN-based power converter. Section IV details the control of the system, including the power converter control loop and the high-level energy management strategy. Section V shows the experimental results obtained with the developed HESS prototype, submitted to different automotive power profiles. Section VI discusses the obtained results and the main limitations and further works of the study are highlighted. Finally, Section VII draws the main conclusions of the study.

II. HYBRID ENERGY STORAGE SYSTEM

This section aims at describing the different components of the developed HESS prototype, specifying successively the main characteristics of the Li-ion battery module, Li-S battery module, and selected coupling topology. Figure 1 shows the battery cells used for the development of both battery modules, while the Table 1 summarizes the characteristics at cell and module level.

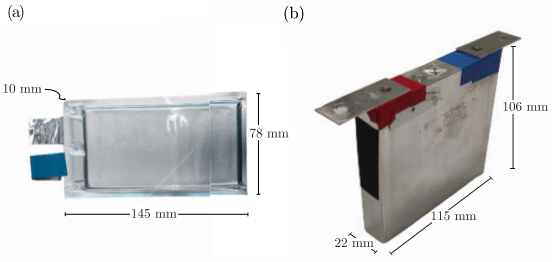

FIGURE 1. Commercial battery cells used for the HESS: (a) Li-S pouch cells, and (b) Prismatic LTO Li-ion cell.

A. Li-S BATTERY MODULE

As previously mentioned, the Li-S technology which combines Li-metal anode with a sulfur-based cathode, was selected to increase the energy density and specific energy of the HESS. Commercial pouch cells [see Fig. 1(a)], were used to develop the Li-S module. Although such cells are early commercial products of a technology under development, they already present increased energy characteristics compared to state-of-the-art commercial Li-ion technology. It is noteworthy that the nominal capacity of 14.7 Ah indicated in Table 1 corresponds to the capacity extracted through 0.2 C discharge. Discharging curves obtained with these cells (from laboratory tests and represented in datasheet) reveal important capacity decreases for increasing C-rates.

The developed Li-S module consisted of 24 cells connected in series, incorporated within a house-made mechanical packaging frame for laboratory use (see Table 1).

B. Li-ION BATTERY MODULE

The role of the Li-ion component within the developed HESS prototype is to provide power capability to the battery-pack. For this reason, the selected Li-ion cell technology should be oriented to power application. Among the different Li-ion chemistries, the LTO anode is particularly suited for high-power applications [23], due to the reduced formation of Solid Electrolyte Interface (SEI) and dendritic Lithium, which enhance the potential for high rate capability [10].

TABLE 1. Nominal characteristics of the commercial Li-S and Li-ion, at cell and module levels.

Description	Li-S		Li-ion		Unit
	Cell	Module	Cell	Module	
Nominal Voltage	2.15	51.6	2.3	55.2	V
Maximum Voltage	2.6	62.4	2.7	64.8	V
Minimum Voltage	1.9	45.6	1.5	36.0	V
Capacity	14.7°		23•		Ah
Energy	31.6°	758.5°	52.9•	1269.6•	Wh
Specific Energy	371°	237°	96•	81.7•	$Wh.kg^{-1}$
Energy Density	287°	160.7°	202•	126.9•	$Wh.L^{-1}$
Continuous Maximum Discharge C-rate	1		4.35		C (or h^{-1})
Peak Maximum Discharge C-rate	2°°		8.70••		C (or h^{-1})
Weight	85	3200 *	550	15540 *	g
Volume	0.11	4.72 *	0.27	10 *	L

° Discharge @ 0.2 C, 20 ºC, °° 30 s, 50% SOC, 20 ºC
• Discharge @ 1 C, 25 ºC, •• 10 s
* Including module packaging and Battery Management System (BMS).

For this reason, a 23 Ah prismatic cell [see Fig. 1(b)], composed of a LTO anode and Nickel-Manganese-Cobalt (NMC) cathode, was selected for the development of the Li-ion module to be included in the HESS battery-pack. In order to compose the battery module, 24 cells were connected in series (see Table 1).

C. HYBRIDIZATION TOPOLOGY

Several hybridization topologies were proposed in the literature to combine energy storage systems, involving different coupling methods with the load system and between both storage systems [4], [24]. In EV applications, the HESS is typically connected with the electric engine by a DC-AC converter [25]. Moreover, the connection between both storage systems could be broadly classified between passive, active or semi-active (cascade) coupling architectures [4].

On the one hand, passive architectures imply direct connection between the storage systems, without any conversion stage. This allows to save the cost and power losses related to power converters. For EV application, removing power converters also implies to increase the energy density and specific energy of the HESS. Nevertheless, passive architectures do not permit to control the power demand for each storage system, leading to non-optimal operation and accelerated degradation of each individual battery system. The failure of one battery could also affect the other one and compromise the performance of the whole system [4], [24].

On the other hand, active architectures typically include DC-DC power converters associated to each individual storage system before the DC-AC conversion stage to the engine. This makes the implementation of advanced energy management strategies possible, as the power demand of each storage system could be actively controlled in accordance with its intrinsic characteristics and optimal operation boundaries. Nevertheless, this is achieved at the expense of increased system costs, weight, volume, and power losses. Finally, semi-active (cascade) architectures consist on coupling both storage systems in series, introducing a DC-DC power conversion stage between them. Such an approach represents a suitable trade-off for EV applications, providing enough flexibility to directly control the power demand of one storage system, and ensuring at the same time reduced system costs, weight, volume, and power losses compared to active solutions [26].

Within the context of this research, a semi-active topology was designed, as illustrated in Fig. 2. In fact, the early maturity stage of the Li-S cell technology requires careful operation to minimize degradation [27]. This makes the use of a power converter necessary for optimal control of the Li-S system. In order to minimize the weight, volume and power losses of the system, and do not compromise the high energy density and specific energy obtained through Li-S cells integration, a high-performance power converter is required.

III. BIDIRECTIONAL DC-DC CONVERTER

Considering characteristics of batteries presented in Table 1, specifications of the power converter are derived in Table 2. The non-inverting buck-boost converter topology was considered in this work, due to its simplicity and similar battery voltage levels. Fig. 2(b) shows the power converter which is composed of two half-bridge branches interconnected by an inductor. These branches are named as primary and secondary considering a power flow from Li-ion battery to Li-S battery. The non-inverting buck-boost converter can operate in different operation modes [15], [28]. Operation modes of the power converter are related to voltage relation, along with primary ($\delta_{1,i}$) and secondary side ($\delta_{2,i}$) duty cycles. In this case study, a *buck or boost* control strategy is considered, with the aim of achieving high-efficiency [15].

This converter is operated in a Continuous Conduction Mode (CCM), avoiding high current stresses and allowing simple linear control [see Fig. 2(c)]. As a result of the required

TABLE 2. DC-DC power converter specifications.

Description	Value	Unit
Buck-branch voltage - $V_{\mathrm{Li-ion}}$	36-64.8	V
Boost-branch voltage - $V_{\mathrm{Li-S}}$	45.6-62.4	V
Peak power - $\hat{P}_{\mathrm{T}}$	1	kW
Relative current ripple - ΔI	<0.2	
Voltage ripple - Δv	<0.2	
Switching frequency - f_{s}	300	kHz
Interleaved modules - N_{p}	2	

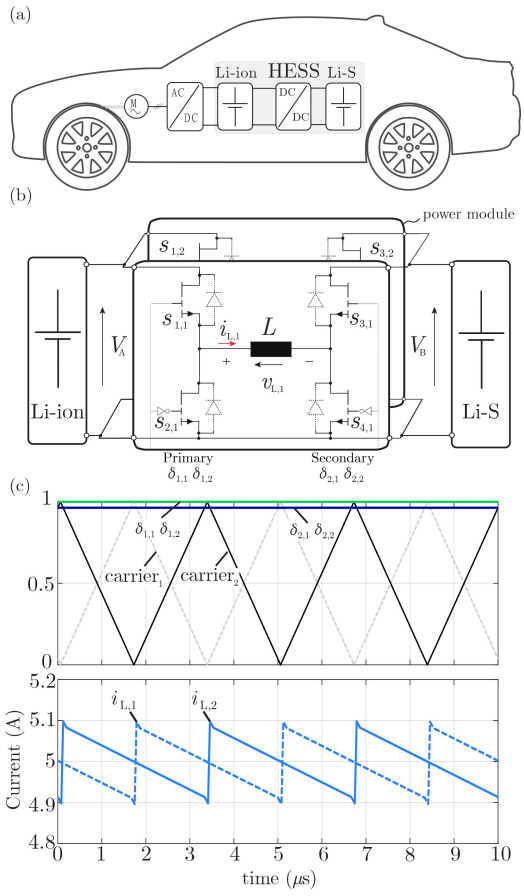

FIGURE 2. Semi-active HESS for EV: (a) EV power distribution system, (b) interleaved bidirectional buck-boost converter based on GaN devices for Li-S and Li-ion semi-active hybridization and (c) buck-boost key waveforms, interleaved carriers, branches duty cycles ($\delta_{1,1}, \delta_{2,1}, \delta_{1,2}, \delta_{2,2}$) and inductors currents ($i_{\mathrm{L},1}, i_{\mathrm{L},2}$) (Boost mode 48/49V, 5A/module).

current ripple and power level, interleaved solution is presented as the preferred choice. Fig. 2(c) illustrates the key waveforms under CCM operation in one-switching period. With the interleaving solution the current ripple is reduced N_{p} number of interleaved DC-DC power modules, as it is shown in Fig. 2(c). More details of the design and operation principles were already discussed in the literature [15], [28].

Thus, the aim of this section is to evaluate the performance of the designed power converter in comparison to Si-based solution. Besides, experimental measurements are included in order to validate the performance of the presented solution for the HESS requirements.

A. POWER CONVERTER PERFORMANCE

When analyzing the performance of a power converter, semiconductors and inductive components are the major contributors of power losses, volume and weight. Thus, the impact on the performance of these components was modeled, estimating power losses of semiconductors along with weight and volume models. These models are based on updated commercial database for inductive components and heatsinks [15]. The presented approximation models are suitable for general optimization routines, reducing long convergence times, as it is presented in [29] for medium frequency high-power converters.

The performance of the power converter was evaluated considering the following characteristics:

i) Cooling system is based on natural convection;
ii) ceramic capacitors with negligible power losses and volume impact as input and output capacitors;
iii) commercial 200 V Si OptiMOS 3 device (Infineon);
iv) low-voltage GaN power semiconductors (EPC2034);
v) converter output power is rated at 1000 W;
vi) volume and weight estimation without housing.

Fig. 3 presents power losses, volume and weight comparison for Si-based and GaN-based solutions operating at high-switching frequency (300 kHz). GaN devices present lower power losses than Si counterparts. Losses of Si semiconductors begin to be relevant at high-switching frequency and hard-switching operation mode. This power losses increment has a direct impact on the volume and weight of the power converter. This is mainly due to cooling system volume impact, as it is shown in Fig. 3. The increase of switching frequency results on a reduction of the whole GaN-based power converter volume and weight. This is mainly due to low power losses of GaN devices, resulting on a negligible requirement of cooling system (see Fig. 3).

GaN-based power converter achieves a clear improvement in terms of power losses, volume and weight in comparison to conventional Si-based solution, with a reduction of 45% and 51% in volume and weight, respectively.

Regarding the performance of GaN semiconductors, Fig. 4 shows the analytical power losses distribution of every switch of the power converter. For this analysis, similar duty cycles for both branches were assumed ($\delta_1 = \delta_2$), along with a power flow from primary to secondary branch, i.e. from the Li-ion battery to the Li-S module. The use of GaN devices results on low conduction losses due to its low conduction resistance (∼10,mΩ) (see Fig. 4). Besides, switching losses are one of the most differential aspects when comparing to Si-based solutions. GaN-based power converter presents 48% lower switching losses than Si-based converter, for 300 kHz and hard-switching operation mode. However, dead-time losses need to be considered when working at high-switching frequency (see Fig. 4). Indeed, free-wheeling

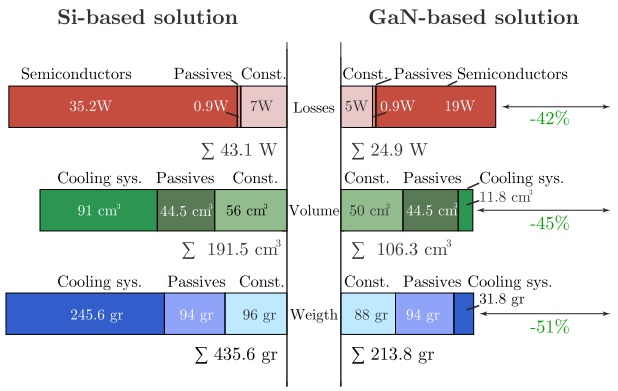

FIGURE 3. Theoretical power converter performance analysis, comparing GaN-based and Si-based solutions in terms of power losses, volume and weight (without housing).

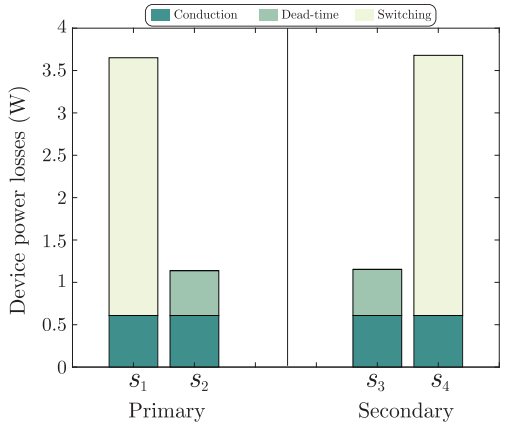

FIGURE 4. Analytical power losses distribution of one power cell based on GaN devices, differing between primary and secondary branches, and considering a power delivery from Li-S to Li-ion.

reverse conduction of GaN devices presents a high reverse voltage drop, resulting in higher dead-time losses than its Si counterparts. Therefore, minimum dead-time selection (50 ns) is relevant in order to minimize this effect.

B. EXPERIMENTAL EVALUATION

Considering the theoretical performance results, a GaN-based experimental prototype was built. Figure 5(a) shows the DC-DC converter that connects the two battery technologies. This converter is comprised by two interleaved power modules, resulting on four half-bridge cells and two inductors, within an aluminum housing, which is used to cool-down the system. Regarding the half-bridge power cell, it is composed of a power board and a conditioning board, as it is depicted in Fig. 5(b). The power converter is based on low-voltage GaN semiconductors, resulting on a design with a reduced size and weight (see Fig. 5).

Additionally, Fig. 6 shows the performance of the power converter in terms of efficiency for bidirectional operation, which was measured with Yokogawa WT500. With this analysis low power losses of the GaN-based power converter is demonstrated, achieving high efficiency even at 300 kHz switching frequency (see Fig. 6). A peak efficiency of 96.5% for the nominal operation is measured, i.e., Li-S 0.2 C current

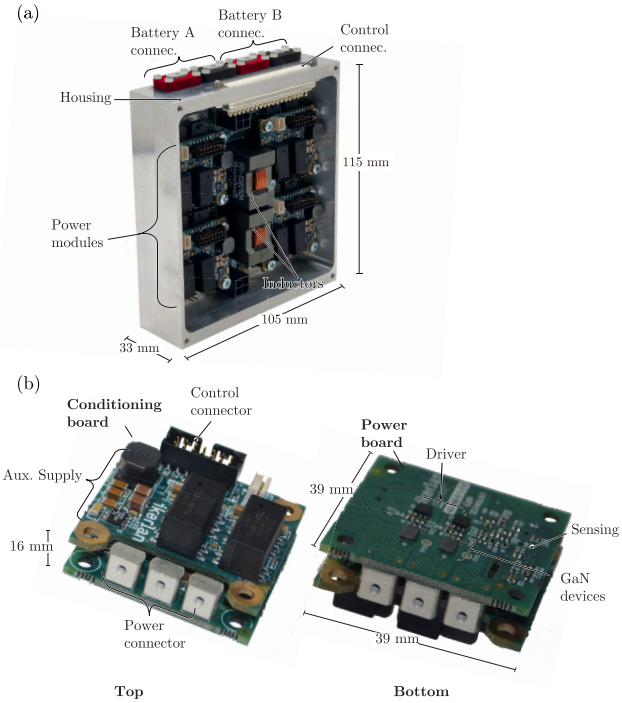

FIGURE 5. Multi-cell bidirectional buck-boost converter for HESS. (a) DC-DC prototype composed by four power cells and two inductors. (b) GaN-based half-bridge power cell conformed by power and conditioning boards.

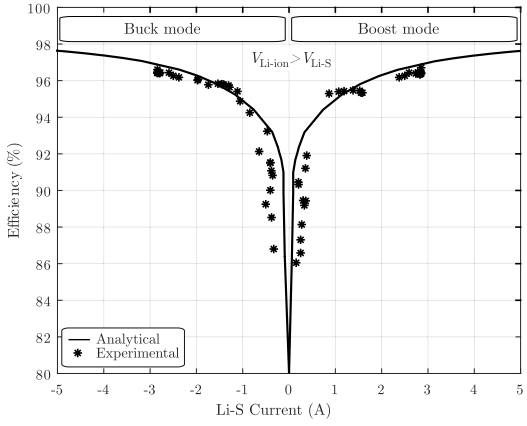

FIGURE 6. Experimental evaluation of the efficiency of the DC-DC power converter working at nominal operating conditions, i.e., Li-S 0.2 C current rate.

rate. Considering $V_{\mathrm{Li-ion}} > V_{\mathrm{Li-S}}$ buck ($I_{\mathrm{Li-S}} < 0$) and boost ($I_{\mathrm{Li-S}} > 0$) modes were evaluated. Symmetrical results were obtained as a consequence of similar power boards used for both branches, and the same is true for $V_{\mathrm{Li-ion}} < V_{\mathrm{Li-S}}$ operating condition.

IV. CONTROL STRATEGY

The control strategy depicted in Fig. 7 was implemented in the HESS prototype, with a bidirectional power delivery control. This control strategy was composed of two main stages: the energy management strategy and the power converter control loop.

On the one hand, for the energy management strategy, a rule-based method was proposed. The current required by

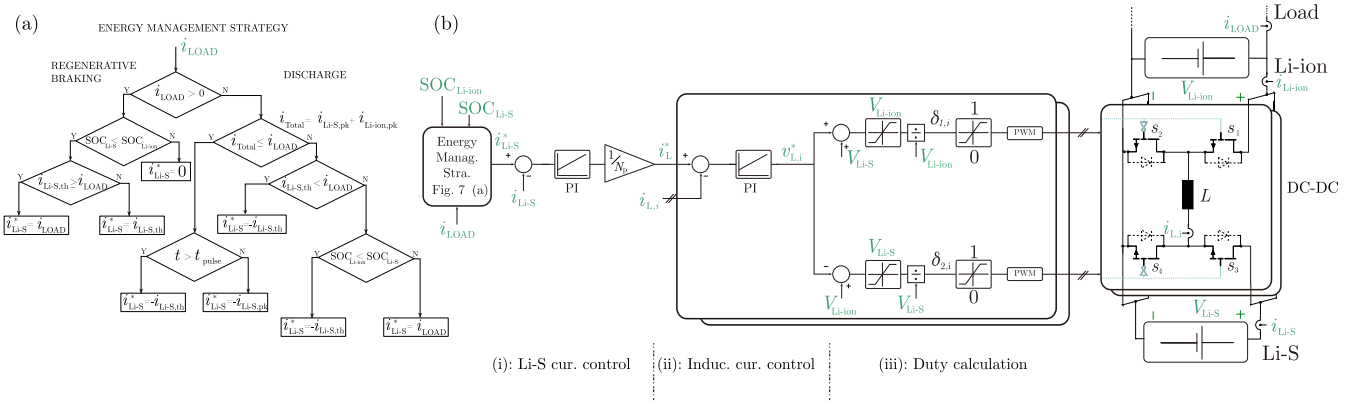

FIGURE 7. HESS control strategy. (a) Flowchart representing the rule-based energy management strategy, being i_{LOAD} the load current; SOC_{Li-S} and SOC_{Li-ion} the average SOC of the Li-S and Li-ion modules respectively; $i_{Li-S,th}$ and $i_{Li-S,pk}$ the defined maximum DC and pulse current thresholds for the Li-S; i_{total} is equal to the sum of $i_{Li-S,pk}$ and the maximum Li-ion pulse current $i_{Li-ion,pk}$; t_{pulse} is the maximum duration for which the Li-S pulse current could be provided; and i^*_{Li-S} is the generated Li-S current reference. (b) Buck-boost converter control strategy, divided in three stages: (i) Li-S current control, obtaining the inductor current reference for interleaving converters $i^*_{L,i}$; (ii) inductor current control, providing inductor voltage $v^*_{L,i}$ and (iii) duty calculation, obtaining primary and secondary duty cycles, $\delta_{1,i}$ and $\delta_{2,i}$ respectively.

the Li-S battery module was defined according to each battery State-of-Charge (SOC), the required output current and current thresholds, resulting from laboratory results in order to optimize the efficiency and lifetime of batteries. On the other hand, for the power converter control loop, a buck-boost control strategy was chosen with an interleaving Pulse Width Modulation (PWM).

A. ENERGY MANAGEMENT STRATEGY

The main goal of the energy management strategy was to decide about how to dispatch the current demand toward the Li-S and Li-ion battery modules, maximizing performances of the HESS and ensuring at the same time a safe and long-lasting operation of both modules [see Fig. 7(a)]. For that purpose, the load current (i_{LOAD}) was measured and then the current demand was obtained.

The current demand was always primarily oriented to the Li-S module, and the maximum current provided by the Li-S system ($i_{Li-S,th}$) was limited to 0.2 C, to maintain a reasonable capacity of the Li-S cells. In fact, according to experimental results, the capacity which could be extracted from such cells drastically decreases for higher C-rates. The remaining current demand was oriented to the Li-ion module, subjected the following restrictions: i) the maximum current provided by the Li-ion system was limited to 4.35 C, in accordance with aging experimental results; ii) this restriction was allowed to lift towards 8.7 C for a maximum duration of 10 s ($i_{Li-ion,pk}$). If the current demand was still not fulfilled, the maximum current provided by the Li-S system was increased ($i_{Li-S,pk}$) even if it was known that it would cost a slight loss of life, but always limited to 1 C, for a maximum duration of 10 s (t_{pulse}).

Additionally, simple module balancing measures were included in the energy management strategy, stating the following: i) if the whole current demand was lower than the maximum current limit set to the Li-S, and if the SOC of the Li-ion module was lower than the SOC of the Li-S module, the Li-S system was pushed to provide the maximum allowed current (0.2 C) to charge the Li-ion system; ii) during the regenerative braking phases, the collected energy was oriented to the system presenting the lowest SOC.

B. CONVERTER CONTROL LOOP

Regarding the power converter control, the implemented control strategy was comprised as follows: i) Li-S battery current control obtaining inductor current reference ($i^*_{L,i}$), in accordance with the number of interleaved modules (N_p); ii) inductor current ($i_{L,i}$), without exceeding the maximum saturation current of the inductor, obtaining the inductor voltage reference ($v^*_{L,i}$); and iii) duty calculation. The duty cycle of each branch was obtained:

$$\delta_{1,i} = \frac{V_{Li-S} + v^*_{L,i}}{V_{Li-ion}}, \tag{1}$$

$$\delta_{2,i} = \frac{V_{Li-ion} - v^*_{L,i}}{V_{Li-S}}. \tag{2}$$

being V_{Li-ion} the voltage of the Li-ion module and V_{Li-S} the voltage of the Li-S module.

Besides, if the converter is operated in buck regime, meaning that $V_{Li-ion} > V_{Li-S}$, the limiter $(0, V_{Li-ion})$ of the secondary branch indicated automatically saturates the duty cycle of secondary bridge to 1, while the duty cycle of the primary bridge-leg can vary freely in [0, 1] interval. On the contrary during boost operation, secondary bridge is responsible for controlling, while primary bridge is automatically clamped at 1. The transition between the buck and the boost modulation branches has no interruptions, achieving a continuous control, as it is depicted in Fig. 8 for a load variation.

V. HESS EXPERIMENTAL EVALUATION

This section describes and discusses the experimental results achieved with the developed HESS prototype submitted to realistic EV driving profiles. Figure 9 shows the general

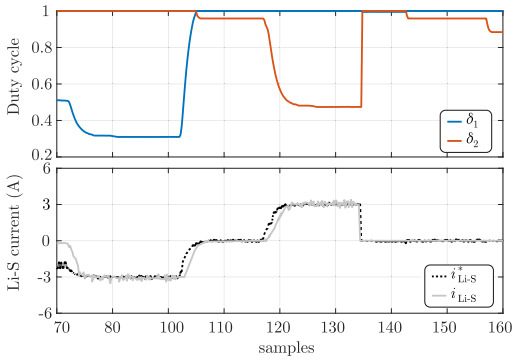

FIGURE 8. Control loop for a bidirectional operating condition. Generated duty cycles (δ_1, δ_2) and Li-S current control response: current reference $i^*_{\text{Li-S}}$ and measured current $i_{\text{Li-S}}$.

schematic of the test bench. For the driving cycle, a battery tester has been used, which can be used as a load or a charger. All the tests have been done at a controlled temperature (20 °C), in a climatic chamber.

The main goals of the experimental study were: i) to analyze the behavior of the HESS prototype under several EV driving scenarios; ii) to verify the increase of energy density and specific energy achieved by combining Li-S and Li-ion technologies under realistic profiles; iii) to identify system limitations and assess how far such HESS prototype would be from a potential use in a commercial EV system.

For this purpose, several experiments were conducted in laboratory. First, the prototype was submitted to a Worldwide Harmonized Test Cycle in Charge Depletion (WLTC-CD) driving profile, which is widely accepted to be representative of an EV motorway driving scenario [30]. Such profile was scaled-down to the developed HESS prototype size, and repeatedly applied until the system was fully discharged. In Section V-A, the profile was first applied to the single Li-ion module, for further comparison purposes. Then, in Section V-B the same profile was applied to the full HESS prototype to analyze the benefits of hybridizing Li-S and Li-ion technologies for EV application. Nevertheless, real-world driving scenarios does not typically imply consecutive sequences of driving cycles. For this reason, in Section V-C, the motorway profile was slightly modified including idle periods between each sequence of WLTC-CD driving cycle. Finally, in Section V-D, the WLTC-CD profile was modified to simulate lower speed and energy-oriented automotive profiles, more representative of urban driving scenarios. All the tests were carried out until the minimum voltage of a battery cell was achieved.

A. SINGLE Li-ION SYSTEM: HIGH-SPEED DRIVING SCENARIO

For comparison purposes, the scaled-down WLTC-CD profile was first applied to the single Li-ion battery module used in the HESS prototype. The cells of the Li-ion module were initialized at 95% SOC.

Figure 10 depicts the results of the experiment, indicating the scaled-down WLTC-CD power profile which was

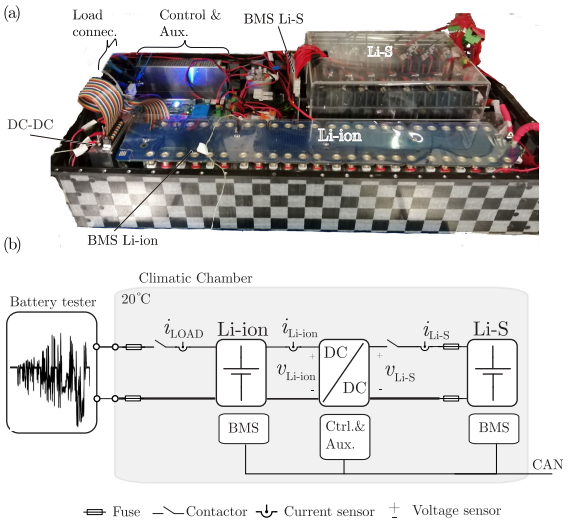

FIGURE 9. Experimental set-up. (a) DBS prototype with control and auxiliary circuits location. (b) General schematic of the laboratory test bench.

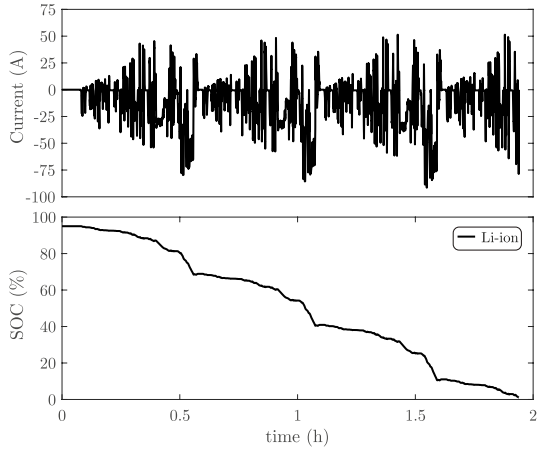

FIGURE 10. Scaled-down WLTC-CD power profile, repeatedly applied to the single Li-ion module (upper graph). Negative values of the current indicate that the battery is discharging, and positive values indicates the battery is charging through regenerative braking. Evolution of the SOC of the Li-ion module is shown in bottom graph.

repeatedly applied to the Li-ion module (upper graph), and the subsequent evolution of the SOC of the module (bottom graph).

The Li-ion module was able to supply 112.94 Wh.L^{-1} and 72.67 Wh.kg^{-1}. The WLTC-CD profile was supplied 3.32 times, calculated as the ratio between the total energy delivered during the test, with respect to the energy corresponding to a single WLTC-CD profile completion. The test was stopped when the module voltage reached the limit discharge voltage value.

B. HESS PROTOTYPE: HIGH-SPEED DRIVING SCENARIO

The high-speed WLTC-CD driving profile was then applied to the whole HESS prototype in the laboratory environment. The cells of both Li-ion and Li-S modules were initialized at 95% SOC.

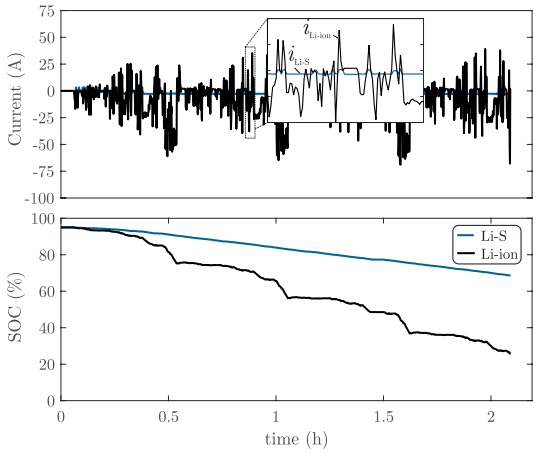

FIGURE 11. Behavior of the HESS under high-speed driving profile. Upper graph: current profile provided by the Li-ion module (black curve) and the Li-S module (blue curve). Bottom graph: SOC evolution of the Li-ion and Li-S cells (respectively in black and blue curves).

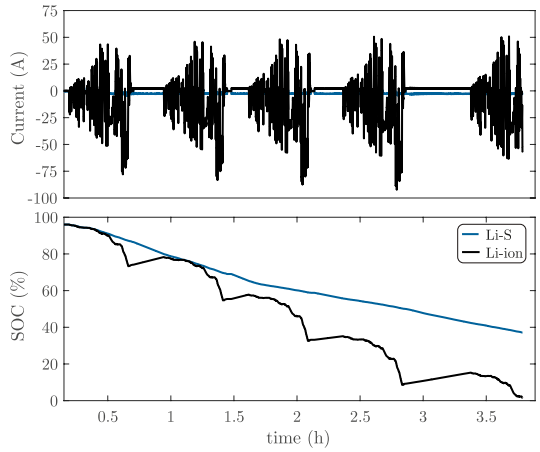

FIGURE 12. Behavior of the HESS under high-speed driving profile with idle periods. Upper graph: current profile provided by the Li-ion module (black curve) and the Li-S module (blue curve). Bottom graph: SOC evolution of the Li-ion and Li-S cells (respectively in black and blue curves).

Under the high-speed driving scenario, the HESS prototype was able to supply 1248.9 Wh. The WLTC-CD profile was supplied 3.67 times, as it is depicted in Fig. 11. In terms of energy density and specific energy, 82.49 $Wh.L^{-1}$ and 64.5 $Wh.kg^{-1}$ were respectively extracted from the HESS, which corresponds to a reduction of -26.96% and -11.25% compared to the results obtained in Section V-A. Such a performance reduction is due to the additional volume and weight of the Li-S module, while the corresponding energy was not fully extractable in this scenario. In this case, the test was stopped because one cell reached the discharge voltage limitation. Notice that, because of cells imbalance, energy remained in both Li-ion and Li-S modules. At the end of the test, 68.57% SOC and 25.81% SOC was remaining respectively in the Li-S and the Li-ion module.

C. HESS PROTOTYPE: HIGH-SPEED DRIVING SCENARIO WITH IDLE PERIODS

Although the scenario implemented in Section V-B is useful to unveil the limitations of the developed HESS prototype, it is noteworthy that in a typical real-world automotive application, driving cycles are not successively applied. In fact, a more realistic operation would involve idle period or pauses between each driving cycle, corresponding to the periods in which the EV would be parked.

For this reason, an additional experiment was conducted intercalating such pauses between each WLTC-CD driving profile. In total, the duration of the idle periods in which the HESS system was not electrically excited was approximately one hour. The results of the applied driving cycle are depicted in Fig. 12.

The WLTC-CD profile was supplied 4.71 times with a total energy of 1603.4 Wh. In terms of energy density and specific energy, 105.9 $Wh.L^{-1}$ and 82.79 $Wh.kg^{-1}$ were respectively extracted from the HESS, which corresponds to a reduction of -6.23% and an increase of $+13.91\%$ compared to the results obtained in Section V-A, for the single Li-ion system. The test was stopped when the Li-ion module was completely discharged. At the end of the test, 37.11% SOC remained in the Li-S module.

D. HESS PROTOTYPE: URBAN DRIVING SCENARIO

The WLTC-CD automotive profile considered in the previous experiments was originally designed to represent high-speed driving ($\sim$120 $km.h^{-1}$) typically related to motorway-type roads. In this section, such power-profile was modified to represent a less power-demanding and smoother conduction, more representative of urban driving scenarios. For this purpose, the automotive power profile used in Section V-B was reduced by a factor of two. In order to maintain an equivalent energy demand, the duration of the automotive profile was also multiplied by a factor of two. Five-minutes short pauses were intercalated between each driving cycle, for cell relaxation purposes.

The HESS prototype was able to supply 1730.2 Wh. The WLTC-CD profile was supplied 5.09 times. The extracted specific energy and energy density were 89.36 $Wh.kg^{-1}$ and 114.28 Wh. L^{-1}, respectively, which represents a $+22.96\%$ and $+1.19\%$ increase compared to the specific energy and energy densities extracted from the Li-ion system in Section V-A. In this experiment, the test was stopped when one Li-S cell of the module reached the discharging voltage limitation (see Fig. 13 and Fig. 14). At the end of the test, the SOC of the Li-ion and Li-S modules were respectively 5.65% and 24.23% SOC.

VI. DISCUSSION LIMITATIONS AND FURTHER WORKS

The main goal of the study was to develop a HESS combining the high-power capability of LTO Li-ion batteries and the high energy density and specific energy of Li-S technology. Table 3 depicts the available energy, energy density and specific energy for the single Li-ion battery module and for the developed HESS prototype. The nominal values of the

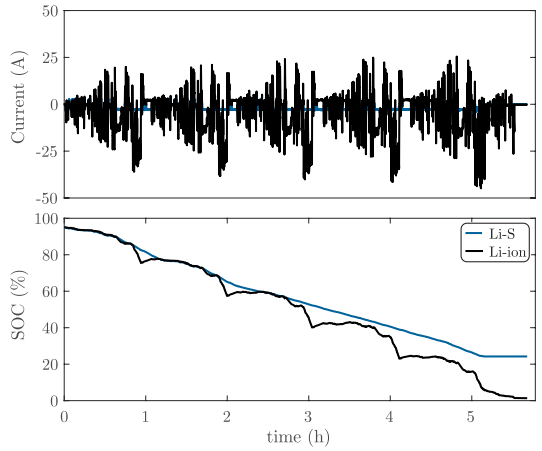

FIGURE 13. Behavior of the HESS under urban driving profile. Upper graph: current profile provided by the Li-ion module (black curve) and the Li-S module (blue curve). Bottom graph: SOC evolution of the Li-ion and Li-S cells (respectively in black and blue curves).

systems are depicted, as well as the energy extracted for the different driving scenarios.

Regarding the energy density and specific energy, two values are differentiated in the Table 3. The first value was calculated considering the weight/volume of the prototype modules and DC-DC converter. Nevertheless, as the developed HESS was a laboratory prototype, the packaging of the Li-ion and Li-S modules was not optimized and could easily be reduced, although this was out of the scope of the study. Therefore, the second value indicated in Table 3 corresponds to the energy density and specific energy calculated considering only the weight/volume of the cells themselves and the DC-DC converter.

As expected, the hybridization of both technologies provided respectively an increase of energy density and specific energy of +5.56% and +28.21%, compared to the single Li-ion system. Besides, discarding the influence of non-optimal packaging of the prototype +8.50% and +32.93% improvement is expected.

Interestingly, the achieved energy density and specific energy values could be relatively reduced compared to energy-oriented Li-ion chemistries, e.g. NMC622 cathodes [31]. Nevertheless, this could potentially be compensated by increasing the gravimetric and volumetric Cell-to-Pack ratios, as demonstrated in [31], which is conceivable for the developed HESS due to GaN-based power converter. Therefore, it is reasonable to state that, optimizing the housing to industrial production quality, the developed HESS concept could be a suitable solution to achieve at the same time high energy density and specific energy at pack level, and an increased power capability provided by LTO anode technology.

Moreover, it is noteworthy that not all the nominal energy is necessarily extractable, and the range of an EV integrating such a HESS would strongly depend on the driving profile. Indeed, applying the WLTC-CD high-speed driving profile (see Section V-B), the experiment was interrupted when the Li-ion module reached the lower voltage limitation, and 68.57% SOC remained in the Li-S module after the end of the experiment. This could be explained by the power restriction applied to the Li-S in the energy management strategy (see Fig. 7), which did not allow the Li-S cell to provide more than a C-rate value of 0.2 C in normal operation. The reason to impose such a restrictive limitation was that the Li-S technology used in the HESS prototype suffers drastic capacity reduction when cycled at higher C-rates. Consequently, due to the power-demanding character of the profile, the Li-ion module was forced to cover most of the demand of the WLTC-CD profile and was discharging faster than the Li-S module (see Fig. 13).

The results from this experiment suggest that the limited power capability of the Li-S technology could potentially be an obstacle for EV application, particularly for a usage involving high-speed and extended range. For such EV usages, it would be necessary to improve the power capability of the Li-S technology. Alternatively, other hybridization approaches could also be considered, involving energy-oriented Li-ion cells and for example future generations of supercapacitors [5].

In a more frequent real-world automotive scenario, when idle periods were intercalated between each driving cycle (see Section V-C), more energy was extracted from the HESS system compared to the results achieved in Section V-B (see Table 3). The reason for that resides in the energy management strategy depicted in Fig. 7 and implemented in the DC-DC of the HESS prototype: during the pauses incorporated in between each automotive driving cycles, the Li-S module was used to charge the Li-ion module, as long as the Li-S module showed a higher SOC state than the Li-ion module. In such a way, the HESS was able to supply respectively an increase of energy density and specific energy of −6.23% and +13.91%, compared to the single Li-ion system (−3.57% and +18.14% discarding the influence of non-optimal packaging of the prototype). It is noteworthy that the energy deliverable by the HESS is strongly related to the duration of the idle period. Although this experiment considered idle periods of approximately 15 minutes, each driving session could be separated by several hours in real-world scenario (e.g., 8 hours during the night and working times). Therefore, the improvement of the delivered energy density and specific energy could be easily increased considering larger pauses, surrounded this way the +5.56% and +28.21% increase obtained with nominal energy values of the modules. This experiment highlights the importance of the energy management strategies regarding the HESS performance. Further works include research on improved energy management strategies based on optimization methods.

Moreover, during the experiment corresponding to the urban driving scenario (Section V-D), the HESS was able to supply additional energy, providing 1730.2 Wh. The experiment was interrupted because one Li-S cell of the module reached the discharging voltage limitation, while 5.65% and 24.23% SOC was remaining in the Li-ion and Li-S modules,

TABLE 3. Energy, energy density and specific energy for the single Li-ion battery module and the HESS prototype. Nominal values and values extracted for the different driving scenarios.

	Unit	Li-ion module		HESS prototype			
		Nominal	Extracted	Nominal	Extracted		
					High-speed	High-speed with idle periods	Urban
Energy	Wh	1269.6	1129.4	2028.1	1248.9	1603.4	1730.2
Energy density	$Wh.L^{-1}$	126.9 *	112.94 *	133.96 *	82.49 *	105.9 *	114.28 *
		195.93 **	174.29 **	212.59 **	130.91 **	168.07 **	181.36 **
Specific energy	$Wh.kg^{-1}$	81.7 *	72.68 *	104.75 *	64.5 *	82.79 *	89.36 *
		96.18 **	85.56 **	127.85 **	78.74 **	101.08 **	109.07 **

* Considering the weight/volume of the Li-ion module, Li-S module and power converter.
** Considering the weight/volume of the Li-ion cells, Li-S cells and power converter.

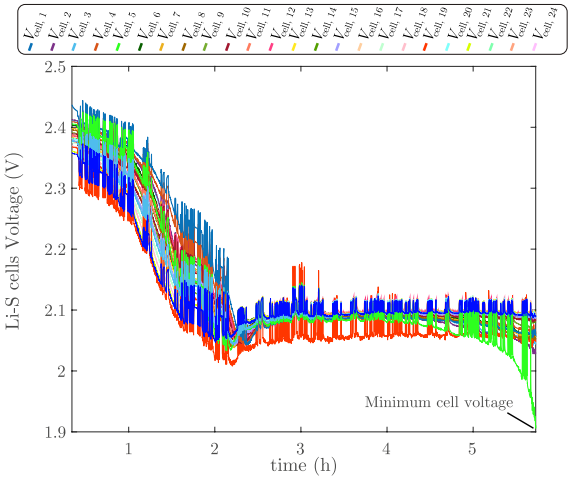

FIGURE 14. Voltage curves obtained during the experiment for the 24 Li-S cells implemented in the module. Each curve corresponds to a specific Li-S cell (V_{cell}).

respectively. Fig. 14 depicts the voltage curves obtained during the experiment for each individual Li-S cell.

The Li-S cell which reached the voltage limitation is clearly recognizable in Fig. 14, and the corresponding voltage curve suggests that the SOC of such cell was lower than the remaining cells in the module. This could be caused by i) a progressive unbalancing trend between the Li-S cells during the experiment, possibly due to intrinsic cell-to-cell discrepancies regarding coulombic efficiency and/or self-discharge rates [32], or ii) a premature aging of such cell compared to the others, leading to a relatively reduced capacity or internal resistance increase [27]. As Li-S cell chemistry is a recent technology which is still under continuous development, there is a clear lack of background on Li-S state estimation methods and analysis tools. This hinders, for now, to clarify the precise reasons behind the accelerated voltage drop of this cell. This should be analyzed in further works.

The performance of the battery at module-level is always limited by the weakest cell, and this is clearly corroborated in this experiment. This highlights the paramount importance of fostering further research on the development of reliable and accurate SOC and State-of-Health (SOH) algorithms for Li-S technology, which in turns could allow making progress on effective balancing strategies tailored to Li-S battery modules.

As energy was remaining in the Li-ion module after the experiment was stopped by Li-S voltage limitation, the profile was applied again to the single Li-ion module, in order to push the HESS prototype until its broadest energy performance limitation. This way, the HESS prototype was able to supply 1781.7 Wh in total. The extracted energy density and specific energy were 117.68 $Wh.L^{-1}$ and 92.02 $Wh.kg^{-1}$ respectively, which represents a +4.21% and +26.62% increase with respect to the energy density and specific energy extracted from the single Li-ion system experiment.

Finally, the low cycle life of Li-S technology reported in literature [2], would also have a significant impact on system behavior. Nevertheless, aging studies remained out of the scope this research and should be investigated in further works.

VII. CONCLUSION

In this study, the development of a hybrid energy storage system was investigated for EV application, with the aim of achieving at the same time an increased energy density, specific energy, and power capability. The system was composed of three key components, namely i) a Li-ion battery module to fulfill high-power requirements; ii) a Li-S battery module to increase the energy density and specific energy of the system, and iii) a GaN-based DC-DC power converter to control and protect the sensitive Li-S system, maintaining at the same time a reduced size and high-efficiency at system level. The GaN-based power converter achieved a clear improvement in terms of power losses, volume and weight in comparison to conventional Si-based solutions, with a reduction of 45% and 51% in volume and weight, respectively.

The developed HESS prototype achieved respectively an increase of energy density and specific energy of +5.56% and +28.21%, compared to a single Li-ion system. Moreover, in order to assess how far such HESS technology would be from potential use in an EV application, the prototype was submitted to several power profiles representing different real-world driving scenarios. The obtained results allowed to identify the main paths for improvement and suggests focusing research efforts on i) working on next-generation Li-S cell technology, especially improving the power capability, ii) further investigations on developing battery models, state algorithms and analysis tools tailored to Li-S chemistry, and iii) continue developing application-oriented energy

management strategies to maximize the performances of current Li-S technology.

REFERENCES

[1] H. Ritchie and M. Roser. (2020). *Co_2 and Greenhouse Gas Emissions*. [Online]. Available: https://ourworldindata.org/co2-and-other-greenhouse-gas-emissions
[2] Z. P. Cano, D. Banham, S. Ye, A. Hintennach, J. Lu, M. Fowler, and Z. Chen, "Batteries and fuel cells for emerging electric vehicle markets," *Nature Energy*, vol. 3, no. 4, pp. 279–289, Apr. 2018.
[3] M. Soltani and S. H. Beheshti, "A comprehensive review of lithium ion capacitor: Development, modelling, thermal management and applications," *J. Energy Storage*, vol. 34, Feb. 2021, Art. no. 102019.
[4] R. Hemmati and H. Saboori, "Emergence of hybrid energy storage systems in renewable energy and transport applications–A review," *Renew. Sustain. Energy Rev.*, vol. 65, pp. 11–23, Nov. 2016.
[5] T. S. Babu, K. R. Vasudevan, V. K. Ramachandaramurthy, S. B. Sani, S. Chemud, and R. M. Lajim, "A comprehensive review of hybrid energy storage systems: Converter topologies, control strategies and future prospects," *IEEE Access*, vol. 8, pp. 148702–148721, 2020.
[6] Poonam, K. Sharma, A. Arora, and S. K. Tripathi, "Review of supercapacitors: Materials and devices," *J. Energy Storage*, vol. 21, pp. 801–825, Feb. 2019.
[7] B. Zhao, R. Ran, M. Liu, and Z. Shao, "A comprehensive review of Li 4 Ti 5 o 12 -based electrodes for lithium-ion batteries: The latest advancements and future perspectives," *Mater. Sci. Eng.: R: Rep.*, vol. 98, pp. 1–71, Dec. 2015.
[8] J. Janek and W. G. Zeier, "A solid future for battery development," *Nature Energy*, vol. 1, no. 9, p. 16141, Sep. 2016.
[9] J. W. Choi and D. Aurbach, "Promise and reality of post-lithium-ion batteries with high energy densities," *Nature Rev. Mater.*, vol. 1, no. 4, p. 16013, Apr. 2016.
[10] H. Zhao, N. Deng, J. Yan, W. Kang, J. Ju, Y. Ruan, X. Wang, X. Zhuang, Q. Li, and B. Cheng, "A review on anode for lithium-sulfur batteries: Progress and prospects," *Chem. Eng. J.*, vol. 347, pp. 343–365, Sep. 2018.
[11] A. Fotouhi, D. J. Auger, K. Propp, S. Longo, and M. Wild, "A review on electric vehicle battery modelling: From lithium-ion toward lithium–Sulphur," *Renew. Sustain. Energy Rev.*, vol. 56, pp. 1008–1021, Aug. 2016.
[12] K. Propp, D. J. Auger, A. Fotouhi, M. Marinescu, V. Knap, and S. Longo, "Improved state of charge estimation for lithium-sulfur batteries," *J. Energy Storage*, vol. 26, Dec. 2019, Art. no. 100943.
[13] G. R. Broday, C. B. Nascimento, E. Agostini, and L. A. C. Lopes, "A bidirectional DC-DC converter for supercapacitors in hybrid energy storage systems," in *Proc. 11th IEEE Int. Conf. Compat., Power Electron. Power Eng. (CPE-POWERENG)*, Apr. 2017, pp. 298–303.
[14] Y. Wang, L. Wang, M. Li, and Z. Chen, "A review of key issues for control and management in battery and ultra-capacitor hybrid energy storage systems," *eTransportation*, vol. 4, May 2020, Art. no. 100064.
[15] A. Avila, A. Garcia-Bediaga, I. Gandiaga, L. Mir, and A. Rujas, "GaN-based DC-DC power converter for hybrid energy storage system," in *Proc. IEEE Vehicle Power Propuls. Conf. (VPPC)*, Nov. 2020, pp. 1–5.
[16] G. Gurjar, D. K. Yadav, and S. Agrawal, "Illustration and control of non-isolated multi-input DC-DC bidirectional converter for electric vehicles using fuzzy logic controller," in *Proc. IEEE Int. Conf. Innov. Technol. (INOCON)*, Nov. 2020, pp. 1–5.
[17] H. J. Ferreira, S. Kouro, C. A. Rojas, N. Muller, and S. Rivera, "Bidirectional partial power DC-DC configuration for Hess interface in EV powertrains," in *Proc. 22nd IEEE Int. Conf. Ind. Technol. (ICIT)*, Mar. 2021, pp. 327–332.
[18] Y. Lei, C. Barth, S. Qin, W.-C. Liu, I. Moon, A. Stillwell, D. Chou, T. Foulkes, Z. Ye, Z. Liao, and R. C. Pilawa-Podgurski, "A 2 kW, single-phase, 7-level, GaN inverter with an active energy buffer achieving 216 W/in^3 power density and 97.6% peak efficiency," in *Proc. IEEE Appl. Power Electron. Conf. Expo. (APEC)*, Mar. 2016, pp. 1512–1519.
[19] M. J. Kasper, L. Peluso, G. Deboy, G. Knabben, T. Guillod, and J. W. Kolar, "Ultra-high power density server supplies employing GaN power semiconductors and PCB-integrated magnetics," in *Proc. 11th Int. Conf. Integr. Power Electron. Syst.*, Mar. 2020.
[20] Z. Song, H. Hofmann, J. Li, X. Han, X. Zhang, and M. Ouyang, "A comparison study of different semi-active hybrid energy storage system topologies for electric vehicles," *J. Power Sources*, vol. 274, pp. 400–411, Jan. 2015.
[21] M. R. Rade, "Design and development of hybrid energy storage system for electric vehicle," in *Proc. Int. Conf. Inf., Commun., Eng. Technol. (ICICET)*, Aug. 2018, pp. 1–5.
[22] V. Shende, K. V. Singh, H. O. Bansal, and D. Singh, "Sizing scheme of hybrid energy storage system for electric vehicle," *Iranian J. Sci. Technol., Trans. Electr. Eng.*, vol. 45, no. 3, pp. 879–894, Mar. 2021.
[23] T. Nemeth, P. Schröer, M. Kuipers, and D. U. Sauer, "Lithium titanate oxide battery cells for high-power automotive applications–electro-thermal properties, aging behavior and cost considerations," *J. Energy Storage*, vol. 31, Oct. 2020, Art. no. 101656.
[24] E. G. Perez, "Hybrid energy storage systems via power electronic converters," Ph.D. dissertation, MGEP, Univ. Mondragón, Mondragón, Spain, 2019. [Online]. Available: https://hdl.handle.net/20.500.11984/1783
[25] A. Emadi, L. J. Young, and K. Rajashekara, "Power electronics and motor drives in electric, hybrid electric, and plug-in hybrid electric vehicles," *IEEE Trans. Ind. Electron.*, vol. 55, no. 6, pp. 2237–2245, Jun. 2008.
[26] X. Gao and L. Fu, "SOC optimization based energy management strategy for hybrid energy storage system in vessel integrated power system," *IEEE Access*, vol. 8, pp. 54611–54619, 2020.
[27] S. Nanda and A. Manthiram, "Lithium degradation in lithium–sulfur batteries: Insights into inventory depletion and interphasial evolution with cycling," *Energy Environ. Sci.*, vol. 13, no. 8, pp. 2501–2514, 2020.
[28] J.-W. Jang, Y.-H. Kim, B.-Y. Choi, Y.-C. Jung, and C.-Y. Won, "Control strategy of bidirectional converter for energy storage system in photovoltaic hybrid modules," in *Proc. Int. Conf. Electr. Mach. Syst. (ICEMS)*, Oct. 2013, pp. 444–449.
[29] A. Garcia-Bediaga, "Optimal design of medium frequency high power converters," Ph.D. dissertation, IEL, Ecole Polytechnique Fédérale de Lausanne, Lausanne, Switzerland, 2014. [Online]. Available: https://infoscience.epfl.ch/record/200158?ln=en, doi: 10.5075/epfl-thesis-6205.
[30] M. Tutuianu, P. Bonnel, B. Ciuffo, T. Haniu, N. Ichikawa, A. Marotta, J. Pavlovic, and H. Steven, "Development of the world-wide harmonized light duty test cycle (WLTC) and a possible pathway for its introduction in the European legislation," *Transp. Res. D, Transp. Environ.*, vol. 40, pp. 61–75, Oct. 2015.
[31] X.-G. Yang, T. Liu, and C.-Y. Wang, "Thermally modulated lithium iron phosphate batteries for mass-market electric vehicles," *Nature Energy*, vol. 6, no. 2, pp. 176–185, Feb. 2021.
[32] G. Plett, *Battery Management Systems: Equivalent-Circuit Methods*, vol. 2. Artech, 2015.

ANDER AVILA received the B.Sc. degree in industrial electronics and the M.Sc. degree in energy and power electronics from the University of Mondragón, Mondragón, Spain, in 2013 and 2015, respectively, and the Ph.D. degree from the University of Oviedo, Gijón, Spain, in 2019. Since 2015, he has been with IKERLAN Technology Research Centre (BRTA), Mondragón, as a Researcher in power electronics area. His current research interests include the design and optimization of power converters for electrical traction, renewable energy, and inductive power transfer and energy storage applications based on wide-bandgap devices.

MATTIN LUCU (Member, IEEE) received the M.Sc. degree in integration of renewable energy sources into the electricity grid from the University of the Basque Country (UPV-EHU), Spain, in 2016, and the Ph.D. degree in data-driven aging models for Li-ion batteries from IKERLAN Technology Research Centre (BRTA), in collaboration with the University of the Basque Country. During his graduate studies, he worked as a Research and Development Intern at EneR-GEA Research Group, ESTIA Engineering School, France, in wind turbine emulation and control, and EDP in the analysis of photovoltaic power insertion in low-voltage distribution networks. His research interests include modeling and control of electrochemical energy storage systems, machine learning applied to battery diagnostic and prognostic algorithms, fleet battery data analytics, and cloud-based battery management.

ASIER GARCIA-BEDIAGA (Member, IEEE) received the B.Sc. degree in electronics from the University of Mondragón, Spain, in 2007, the M.Sc. degree from the Electrical, Electronics, Computer Science, Hydraulics and Telecommunications Engineering School (ENSEEIHT), Toulouse, France, in 2009, and the Ph.D. degree from the Swiss Federal Institute of Technology, Lausanne (EPFL), Switzerland, in 2014. Since 2014, he has been with IKERLAN Technology Research Centre (BRTA), Mondragón, as a Researcher in power electronics area. His research interests include wide bandgap power electronics devices and the design, control, and optimization of hard and soft-switching power converters for railway, storage systems, and inductive power transfer applications.

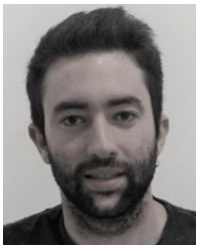

UNAI IBARGUREN received the B.Sc. degree in energy engineering from Mondragón University, Spain, in 2016, and the M.Sc. degree in control in smart grids and distributed generation from the University of the Basque Country (UPV/EHU), Spain, in 2018. In 2018, he joined IKERLAN Technology Research Centre (BRTA), where he is currently working as a Researcher with the Department of Electrical Energy Storage. His research interests include the characterization of electrochemical energy storage systems, and the development of state estimation algorithms for Li-ion batteries and their implementation in battery management systems.

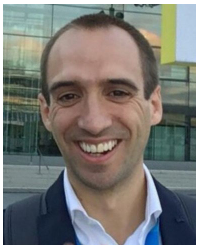

IÑIGO GANDIAGA graduated in physical sciences from the University of the Basque Country (UPV-EHU), Spain, in 2010. He joined IKERLAN Technology Research Centre (BRTA), Mondragón, in 2010. His main activity is focused on electrical storage projects. He has actively participated and led different industrial projects in the last ten years. In addition, he has participated in several projects of the European FP7 and H2020 Program. He is currently the Coordinator of the SENSIBAT Project (H2020 Program). His research interests include the field of analysis of the useful life and state of batteries for electric mobility applications and stationary applications with different storage technologies, namely EDLC, LIC, Li-ion, and post Li-ion. As a result of his research, he has participated in more than ten publications in leading magazines.

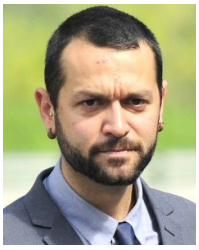

ALEJANDRO RUJAS received the B.Sc. degree in electronics from the University of Mondragón, Spain, in 2004, and the M.Sc. degree in electrical engineering from the Swiss Federal Institute of Technology, Lausanne, Switzerland, in 2007. Since 2007, he has been with IKERLAN Technology Research Centre (BRTA), Mondragón, as a Researcher in power electronics area, and the Leader of the Power Converters Team, since 2016. He has been involved in several industrial and research project related the design and control of power electronics converters for electrical traction, renewable energy, aeronautics, and energy storage applications.